

Reliable Predictions of the Thermochemistry of Boron–Nitrogen Hydrogen Storage Compounds: $B_xN_xH_y$, $x = 2, 3$

Myrna H. Matus, Kevin D. Anderson, Donald M. Camaioni, S. Thomas Autrey, and David A. Dixon*

Department of Chemistry, The University of Alabama, Tuscaloosa, Alabama 35487-0336, and Pacific Northwest National Laboratory, P.O. Box 999, Richland, Washington 99352

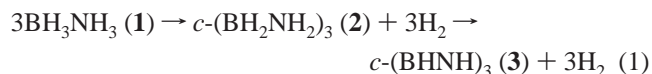
Received: February 2, 2007; In Final Form: February 27, 2007

Thermochemical data calculated using ab initio molecular orbital theory are reported for 16 $B_xN_xH_y$ compounds with $x = 2, 3$ and $y \geq 2x$. Accurate gas-phase heats of formation were obtained using coupled cluster with single and double excitations and perturbative triples (CCSD(T)) valence electron calculations extrapolated to the complete basis set (CBS) limit with additional corrections including core/valence, scalar relativistic, and spin–orbit corrections to predict the atomization energies and scaled harmonic frequencies to correct for zero point and thermal energies and estimate entropies. Computationally cheaper calculations were also performed using the G3MP2 and G3B3 variants of the Gaussian 03 method, as well as density functional theory (DFT) using the B3LYP functional. The G3MP2 heats of formation are too positive by up to ~ 6 kcal/mol as compared with CCSD(T)/CBS values. The more expensive G3B3 method predicts heats of formation that are too negative as compared with the CCSD(T)/CBS values by up to 3–4 kcal/mol. DFT using the B3LYP functional and 6-311+G** basis set predict isodesmic reaction energies to within a few kcal/mol compared with the CCSD(T)/CBS method so isodesmic reactions involving BN compounds and the analogous hydrocarbons can be used to estimate heats of formation. Heats of formation of $c\text{-B}_3\text{N}_3\text{H}_{12}$ and $c\text{-B}_3\text{N}_3\text{H}_6$ are -95.5 and -115.5 kcal/mol at 298 K, respectively, using our best calculated CCSD(T)/CBS approach. The experimental value for $c\text{-B}_3\text{N}_3\text{H}_6$ appears to be ~ 7 kcal/mol too negative. Enthalpies, entropies, and free energies are calculated for many dehydrocoupling and dehydrogenation reactions that convert BNH_6 to alicyclic and cyclic oligomers and $\text{H}_2(\text{g})$. Generally, the reactions are highly exothermic and exergonic as well because of the release of 1 or more equivalents of $\text{H}_2(\text{g})$. For $c\text{-B}_3\text{N}_3\text{H}_{12}$ and $c\text{-B}_3\text{N}_3\text{H}_6$, available experimental data for sublimation and vaporization lead to estimates of their condensed phase 298 K heats of formation: $\Delta H_f^\circ[c\text{-B}_3\text{N}_3\text{H}_{12}(\text{s})] = -124$ kcal/mol and $\Delta H_f^\circ[c\text{-B}_3\text{N}_3\text{H}_6(\text{l})] = -123$ kcal/mol. The reaction thermochemistries for the dehydrocoupling of $\text{BNH}_6(\text{s})$ to $c\text{-B}_3\text{N}_3\text{H}_{12}(\text{s})$ and the dehydrogenation of $c\text{-B}_3\text{N}_3\text{H}_{12}(\text{s})$ to $c\text{-B}_3\text{N}_3\text{H}_6(\text{l})$ are much less exothermic compared with the gas-phase reactions due to intermolecular forces which decrease in the order $\text{BNH}_6 > \text{cyclo-B}_3\text{N}_3\text{H}_{12} > \text{cyclo-B}_3\text{N}_3\text{H}_6$. The condensed phase reaction free energies are less negative compared with the gas-phase reactions but are still too favorable for BNH_6 to be regenerated from either $c\text{-B}_3\text{N}_3\text{H}_{12}$ or $c\text{-B}_3\text{N}_3\text{H}_6$ by just an overpressure of H_2 .

Introduction

There is substantial interest in the development of hydrogen-based fuel cells as a power source which is suitable for use in the transportation sector, environmentally friendly, and not dependent on petroleum as a feedstock. A critical issue with hydrogen as a fuel for use in on-board transportation systems is the need for efficient chemical H_2 storage materials which have a ready release/uptake of H_2 .¹ Borane amine derivatives have been known for a number of years,^{2–4} and there are a number of efforts currently focused on the use of amine boranes for H_2 storage.^{5–8} For example, borazane, BH_3NH_3 (**1**), has received attention due to its high gravimetric and volumetric density of hydrogen and can release covalently bound hydrogen at the low temperatures required for practical implementations. Decomposition of **1** in the solid state to yield an aminoborane polymer and hydrogen is reported to be exothermic by about 5 kcal/mol.⁵ In solution, borazane thermally decomposes to yield hydrogen and cyclotriborazane, $c\text{-B}_3\text{N}_3\text{H}_{12}$ (**2**).^{4c} With further heating, cyclotriborazane decomposes to yield more hydrogen

and borazine, $c\text{-B}_3\text{N}_3\text{H}_6$ (**3**),^{4c,9} as outlined in eq 1.



As shown in Figure 1, these compounds are intermediates on the way to produce solid BN with a graphitic type structure.

The energetics for dehydrogenation of **1** and **2** in the gas and condensed phases are of interest for developing schemes for the release of H_2 and the regeneration of ammonia borane in these hydrogen storage compounds, and thus the thermodynamic properties of amine borane compounds are of critical importance. Wolf and Baumann have determined the standard heat of formation (ΔH_f°) and entropy for solid **1**.¹⁰ Dixon and Gutowski⁶ calculated ΔH_f° (**1**) to be -13.5 kcal/mol in the gas phase using accurate ab initio electronic structure approaches. Data for **3** in the gas (1 bar, 298 K) and liquid phases are available from standard sources (see Table 1).^{11,12} These data allow a determination of the standard enthalpy of reaction for

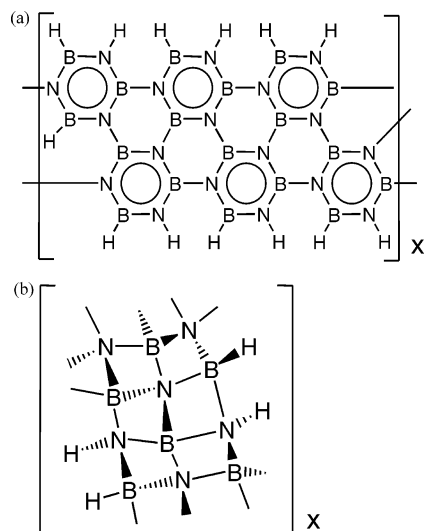


Figure 1. BN structures: (a) graphitic type and (b) diamonoid type.

TABLE 1: Thermodynamic Properties of BN Compounds in Different Phases at 298 K

compd	phase	ΔH_f° 298 K, kcal/mol	S° 298 K, cal/(mol·K)	source
1	gas	-13.5 ± 1.0	57.1	ref 6
1	solid	-36.6 ± 2.4	23.0	ref 5 (S°), ref 10 (ΔH_f°)
2	gas	-96.6 ± 1.0	79.3	this work
2	solid	-120.5 ± 4	21.0	this work (ΔH_f°), ref 13 (S°)
3	gas	-121.9 ± 3		ref 11
3	liquid	-129.0 ± 3	47.7	ref 11 (ΔH_f°), ref 12 (S°)
3	gas	-115.5 ± 1.0	68.7	this work
3	liquid	-122.6 ± 1.1		this work
3	solid	-123.6 ± 1.6		this work

the overall reaction (**1** \rightarrow **3**) at 298 K: $\Delta H_f^\circ = -81.4$ kcal/mol (of **3**) in the gas phase, which is reduced to $\Delta H_f^\circ = -19.2$ kcal/mol (of **3**) to convert pure solid **1** to pure liquid **3**. These data show that intermolecular forces acting in the condensed phase substantially affect the thermochemistry for hydrogen release. Compound **2**, like **1**, is a solid at room temperature and, in addition to gas-phase energies and entropies, other thermochemical information will be needed for the condensed phases. Little experimental data exists to determine the relative stability of **2**. Leavers et al.¹³ measured the equilibrium vapor pressure of solid **2**. By combining these data with high accuracy ab initio calculations of the gas-phase thermochemistry, we can then predict the thermochemical stability of **2** in the solid phase. In addition, the heat of formation of **3** in the gas-phase needs to be re-examined on the basis of high accuracy electronic structure methods.

Production of **2** from three of **1** may proceed through the dimer **4** (Figure 2) so the heat of formation of this compound has been calculated. Production of **3** from **2** can involve a number of ring intermediates, and there are no thermochemical data available for such species. Thus, we also present high level predictions of the gas-phase heats of formation of $B_3N_3H_y$, $y = 8$ and 10, compounds **5**, **6**, and **7** in Figure 2.

Besides the formation of graphitic BN from ring structures (Figure 1a), one can also proceed through linear structures leading to the formation of a ring containing BN with a diamonoid type structure as shown in Figure 1b. We have thus calculated the heats of formation of a number of linear $B_2N_2H_y$ and $B_3N_3H_y$ chains as shown in Figure 2. These types of chains are also relevant to a cationic chain mechanism as recently described.¹⁴

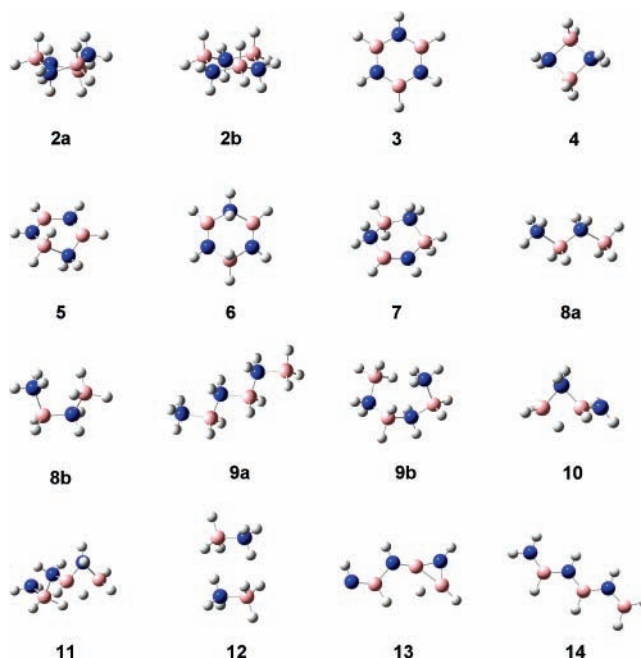


Figure 2. MP2 optimized molecular structures: **2a**, c - $B_3N_3H_{12}$ or cyclotriborazane in twist-boat conformation; **2b**, c - $B_3N_3H_{12}$ or cyclotriborazane in chair conformation; **3**, c - $B_3N_3H_6$ or borazine; **4**, c - $B_2N_2H_8$ or cyclodiborazane; **5**, c - $B_3N_3H_8$ or 5,6-dihydroborazine (could also be named 1,2-dihydroborazine); **6**, c - $B_3N_3H_8$ or 1,4-dihydroborazine; **7**, c - $B_3N_3H_{10}$ or 3,4,5,6-tetrahydroborazine (could also be named 1,2,3,4-tetrahydroborazine); **8a**, $BH_3NH_2BH_2NH_3$ or diborazine in linear conformation; **8b**, $BH_3NH_2BH_2NH_3$ or diborazine in twisted conformation; **9a**, $BH_3(NH_2BH_2)_2NH_3$ or triborazane in linear conformation; **9b**, $BH_3(NH_2BH_2)_2NH_3$ or triborazane in twisted conformation; **10**, $(BH_2NH_2)_2$ or diaminoborane; **11**, $(BH_2NH_2)_3$ or triaminoborane; **12**, $(BH_3NH_3)_2$, head-to-tail borazane dimer; **13**, $(BHNH)_3$ linear structure; **14**, $BH_2(NHBH)_2NH_2$ linear structure. Boron is in pink; nitrogen is in blue.

Computational Approach

We have been involved in developing an approach to the prediction of thermodynamic properties to chemical accuracy based on coupled cluster with single and double excitations and perturbative triples (CCSD(T)) valence electron calculations¹⁵ extrapolated to the complete basis set (CBS) limit with additional corrections.¹⁶ We use such an approach here as we have used for other chemical hydrogen storage systems. The calculations were performed by using the Gaussian 03,¹⁷ MOLPRO 2006,¹⁸ and NWChem¹⁹ suites of programs. The calculations were done on a variety of computers including the Cray XD-1 computer at the Alabama Supercomputer Center, a PQS Opteron computer at the University of Alabama, and the ~ 2000 processor HP Linux cluster in the Molecular Science Computing Facility at the William R. Wiley Environmental Molecular Sciences Laboratory at the Pacific Northwest National Laboratory.

We first describe highly accurate calculations based on the CCSD(T)/CBS extrapolations. The augmented correlation consistent basis sets aug-cc-pVnZ ($n = D, T, Q$), were used for many of the calculations,²⁰ and, for brevity, the basis set names are shortened to aVnZ. The geometries were initially optimized using density functional theory (DFT) with the hybrid B3LYP exchange-correlation functional²¹ in conjunction with the DZVP2 basis set.²² Starting from the DFT geometries, we then optimized the geometries at the MP2/cc-pVTZ level. This level of calculation was also employed for the prediction of the harmonic vibrational frequencies for use in thermal corrections and for the zero point energy (ZPE) calculations. A scaling factor is needed for the zero point energies to correct the harmonic

TABLE 2: Optimized MP2/cc-pVTZ Bond Lengths (Å) and Bond and Dihedral Angles (Degree) for B₃N₃H₆ and B₃N₃H₁₂

	B ₃ N ₃ H ₁₂		B ₃ N ₃ H ₆	
	twist-boat (2a) this work	chair (2b) this work	exptl ^a	planar (3) this work
r_{BN}	1.5838, 1.5938, 1.5932	1.5887	1.4355 ± 0.0021	1.4307
r_{BH}	1.2047, 1.2057, 1.2063	1.2088, 1.2006	1.258 ± 0.014	1.1910
r_{NH}	1.0144, 1.0147, 1.0156	1.0161, 1.0165	1.050 ± 0.012	1.0059
$\angle\text{BNB}$	114.60, 116.08	117.54	121.1 ± 1.2	123.07
$\angle\text{NBN}$	106.08, 105.70	106.85	117.7 ± 1.2	116.93
$\angle\text{BNH}$	110.43, 110.22, 110.14, 107.92, 107.87, 107.59	106.30, 110.74		118.46
$\angle\text{NBH}$	108.36, 108.24, 108.05, 110.03, 109.94, 109.94	109.43, 108.42		121.54
$\angle\text{BNBN}$	−34.30, 67.34 −30.02	−52.82		0.00
$\angle\text{NBNB}$	−34.31, 67.34, −30.00	52.82		0.00
$\angle\text{BNBH}$	83.66, −48.50, 85.60, −151.11, −173.43, −149.84	−171.21, 63.85		180.00
$\angle\text{NBNH}$	90.99, 92.54, −57.85, −154.52, −153.87, −172.47	171.66, −75.82		180.00

^a Reference 42.

frequencies to anharmonic values and any other errors in the calculated frequencies. Because there are issues with the analysis of the experimental spectrum for B₃N₃H₆ as discussed below and because there are no experimental values for B₃N₃H₁₂, we used a scale factor of 0.984 for B₃N₃H₆ from the average of the MP2/cc-pVTZ harmonic frequencies and the experimental fundamentals²³ for the isoelectronic molecule C₆H₆ and a scale factor of 0.980 for B₃N₃H₁₂ obtained from the average of the MP2/cc-pVTZ harmonic frequencies and the experimental fundamentals for the isoelectronic molecule C₆H₁₂.²³ These structures and values were used in calculating the entropies. For the ring molecules **4**, **5**, **6**, and **7**, we used 0.980 as the scale factor to obtain the zero point energies, For **8**, **9**, **10**, and **11**, a scale factor of 0.965, obtained from the MP2/cc-pVTZ ZPE correction and that obtained from ref 6 for BH₃NH₃, was used. For **13** and **14**, a scale factor of 0.974, obtained from the MP2/cc-pVTZ ZPE correction and that obtained from ref 6 for BH₂NH₂, was used. For **12**, a scale factor of 0.968, obtained from the MP2/aug-cc-pVTZ ZPE correction and that obtained from ref 6 for BH₃NH₃, was used.

The MP2/VTZ geometries were used in single point CCSD-(T)/aVnZ calculations for n = D, T, Q. The CCSD(T) total energies were extrapolated to the CBS limit by using a mixed exponential/Gaussian function of the form

$$E(n) = E_{\text{CBS}} + A \exp[-(n - 1)] + B \exp[-(n - 1)^2] \quad (2)$$

with $n = 2$ (aVDZ), 3 (aVTZ), and 4 (aVQZ), as proposed by Peterson et al.²⁴ The CCSD(T) calculations for open-shell atoms were carried out at the R/UCCSD(T) level. In this approach, a restricted open shell Hartree–Fock (ROHF) calculation was initially performed, and the spin constraint was relaxed in the coupled cluster calculation.^{25–27}

Core–valence corrections, ΔE_{CV} , were obtained at the CCSD-(T)/cc-pwCVTZ level.²⁸ Scalar relativistic corrections, ΔE_{SR} , which account for changes in the relativistic contributions to the total energies of the molecule and the constituent atoms, were included at the CI-SD (configuration interaction singles and doubles) level of theory using the aug-cc-pVTZ basis set. ΔE_{SR} is taken as the sum of the mass-velocity and one electron Darwin (MVD) terms in the Breit–Pauli Hamiltonian.²⁹ Most

calculations using available electronic structure computer codes do not correctly describe the lowest energy spin multiplet of an atomic state as spin–orbit in the atom and is usually not included. Instead, the energy is a weighted average of the available multiplets. For N in the ⁴S state, no spin–orbit correction is needed, but a correction of 0.03 kcal/mol is needed for B, taken from the excitation energies of Moore.³⁰

The total atomization energy (ΣD_0 or TAE) of a compound is given by the expression

$$\Sigma D_0 = \Delta E_{\text{elec}}(\text{CBS}) - \Delta E_{\text{ZPE}} + \Delta E_{\text{CV}} + \Delta E_{\text{SR}} + \Delta E_{\text{SO}} \quad (4)$$

By combining our computed ΣD_0 values with the known heats of formation at 0 K for the elements ($\Delta H_f^\circ(\text{N}) = 112.53 \pm 0.02$ kcal mol^{−1}, $\Delta H_f^\circ(\text{B}) = 136.2 \pm 0.2$ kcal mol^{−1}, and $\Delta H_f^\circ(\text{H}) = 51.63$ kcal mol^{−1}),¹¹ we can derive ΔH_f° values for the molecules under study in the gas phase. The value for $\Delta H_f^\circ(\text{B})$ has only recently been revised. The older JANAF value was 132.6 ± 2.9 kcal/mol (133.8 at 298 K),¹¹ while the newer value is 136.2 ± 0.2 kcal/mol (137.7 at 298 K) which we have used.³¹ To obtain the heats of formation at 298 K, we followed the procedure by Curtiss et al.³²

Besides the molecules described above, we are interested in larger boron–nitrogen–hydrogen compounds. Thus, we need computationally cheaper approaches to treat larger rings and chains. We have thus performed G3(B3)³³ and G3(MP2)³⁴ calculations on these compounds and benchmarked the results against the additive CCSD(T)/CBS approach described above. Because of the broad use of the computationally efficient DFT approaches, we have performed DFT calculations with the commonly used B3LYP functional³⁵ and the 6-311+G** basis set.³⁶ Entropies and thermal corrections to 298 K, 1 atm, for these DFT calculations were calculated from unscaled frequencies.

Results and Discussion

Molecular Geometries. The optimized MP2/cc-pVTZ geometries for the two forms of B₃N₃H₁₂ (twist boat, **2a**, and chair, **2b**, Figure 2) and B₃N₃H₆ (structure **3** in Figure 2) are shown in Table 2. In the gas phase, the twist-boat conformer **2a** is more stable than the chair conformer by 1.1 kcal/mol (ΔH),

TABLE 3: Dipole Moments at Different Levels of Calculation (Debyes) for $B_xN_xH_y$ Compounds

molecule	dipole moment			
	B3LYP/ DGDZVP2	B3LYP/ 6-311+G**	HF from G3MP2	HF/ cc-pVTZ
2a	1.214	1.244	1.385	1.415
2b	3.565	3.595	3.826	3.852
3	0.000	0.000	0.000	0.000
4	0.000	0.000	0.000	0.000
5	3.353	3.301	3.586	3.619
6	5.042	4.834	5.051	4.910
7	3.725	3.760	4.323	4.326
8a	10.888	10.764	10.769	10.862
8b	4.208	4.227	4.421	4.308
9a	16.864	16.686	16.745	16.846
9b	1.979	1.919	1.940	1.754
10	2.370	4.999 ^a	4.722 ^a	1.947
11	6.188	6.073	6.151	6.261
12	0.000	0.000	0.000	0.000
13	13.654 ^b	13.864 ^b	13.376	13.090
14	3.951	3.786	3.292	3.406

^a B3LYP/6-311+G* and G3MP2 optimizations give a different geometry than B3LYP/DZVP2 and MP2/cc-pVTZ, where the B–H–B bridge is no longer present. ^b B3LYP/DZVP2 and B3LYP/6-311+G* optimizations give a different geometry than G3MP2 and MP2/cc-pVTZ, where the B–H–B bridge is no longer present.

whereas the free energy is 1.9 kcal/mol showing more conformational flexibility in the twist-boat structure. This contrasts with cyclohexane, for which the twist-boat conformer is 5.5 kcal/mol less stable than the chair conformer.^{37,38} Solid **2** exists in the chair form,³⁹ **2b**, presumably because of enhanced stabilization from dipole–dipole interactions. We compare the calculated chair structure to that from the crystal structure. The calculated BN bond distances are in excellent agreement with the experimental values, and the calculated value of 0.013 Å is longer than the average experimental value of 1.576 Å. The calculated NBN bond angle is 106.8°, less than 0.5° smaller than the average experimental value of 107.2°. The calculated BNB bond angle of 117.5° is 1.6° larger than the experimental value of 115.9°. The calculated HBH angle of 113.4° is in agreement with the experimental value of 111.7°, and the calculated HNH of 105.3° is in agreement with the experimental value of 105.2°. One cannot directly compare the N–H and B–H bond distances because of the foreshortening due to the X-ray analysis.⁴⁰ The geometry parameters for the twist-boat structure are similar to those for the chair.

The gas-phase dipole moments (see Table 3) for the chair and twist-boat conformations of **2** are calculated to be 3.6 and 1.2 debyes, respectively, at the B3LYP level. Levers et al.¹³ measured the dipole moment in 1,4-dioxane ($\epsilon = 2.2$) to be 3.2 D. Given that the value is closer to that for the chair, we estimate that in the dioxane solution, **2** is predominantly in the chair conformation. In later work, Levers and Taylor measured the dipole moment of **2** in 1,4-dioxane and obtained 2.69 ± 0.11 D.⁴¹ Assuming that all of the molecules of **2** are in the chair conformation, they estimated the gas-phase dipole moment to be 2.42 ± 0.16 D. On the basis of our gas-phase results, their second set of results suggests that, in 1,4-dioxane, both conformers are present in about equal amounts.

There are additional chain-like isomers of the trimer (BH_2NH_2)₃. One of these has a bridging H and bridging NH₂, as shown in **11** in Figure 2. A linear (BH_2NH_2)₃ structure does not dissociate but does have an imaginary frequency corresponding to 87.1i cm⁻¹ and a range of B–N distances from 1.46 to 1.87 Å. For **11**, the B–N distances range from 1.50 to 1.70 Å; the B–H distances from the bridge are both 1.33 Å,

and the BHB bond angle is 90.7°. Structure **11** is 33.8 kcal/mol less stable than twist-boat **2**. Structure **11** has a higher dipole moment than **2** so it may be better stabilized in polar media.

The molecule *c*-B₃N₃H₆ has *D*_{3h} symmetry with all equal B–N bond distances. The calculated B–N bond distance for **3** is in excellent agreement with the experimental distance from electron diffraction.⁴² The calculated N–H bond distance is 1.0114 Å at the MP2/cc-pVTZ level as compared to the experimental value of 1.0116 Å in NH₃.⁴³ For comparison, the BH distance in BH₃ at the CCSD(T)/aug-cc-pVQZ level is calculated to be 1.1900 Å which should be an excellent estimate of the B–H distance. The calculated value for BH₃ at the MP2/cc-pVTZ level is 1.1869 Å, in excellent agreement with the CCSD(T) value suggesting that our calculated B–H and N–H bond distances for B₃N₃H₆, **3**, are good to better than 0.01 Å.

A chain-like isomer of (BHNH)₃, **13** in Figure 2, has *C*_s symmetry with B–N distances ranging from 1.34 to 1.60 Å. Similar to **10** and **11**, **13** has a distorted BHB bridge with B–H distances of 1.29 and 1.45 Å, and a BHB bond angle of 83.1°. This bridged structure was obtained in the G3MP2 and MP2/cc-pVTZ optimizations; however, it was not obtained at the B3LYP/DZVP2 and B3LYP/6-311+G** DFT levels, where an optimized geometry similar to polyacetylene was found. Structure **13** is very high in energy, 135.9 kcal/mol above **3**.

Figure 2 shows all of the B–N structures optimized at the MP2/cc-pVTZ level except for the BH₃NH₃ head-to-tail hydrogen-bonded dimer, which was optimized at the MP2/aug-cc-pVTZ level. Important geometry parameters for the B–N framework are given in Table 4. The molecule *c*-B₂N₂H₈ (**4** in Figure 2) exhibits a planar B–N–B–N structure with *D*_{2h} symmetry with B–N distances of 1.606 Å (slightly larger than in **2**), BNB bond angles of 87.9°, and NBN bond angles of 92.1°. Optimizations initiated from a nonplanar B–N–B–N ring led to a planar ring structure. Thus, *c*-B₂N₂H₈ differs from cyclobutane, which is nonplanar.⁴⁴ We can compare the calculated geometry of **4** with that determined in the X-ray crystal structure of the dimethylamino derivative.⁹ The calculated distance is 0.01 Å longer than the experimental value. The calculated NBN and BNB bond angles are closer to 90° than in experiment, and the calculated bond angles show the same behavior with the former less than 90° and the latter greater than 90°.

There is a second structure with B₂N₂H₈. It has a bridging H, a bridging NH₂, and a terminal NH₂ as shown in **10** in Figure 2. Linear BH₂NH₂BH₂NH₂ is unstable as attempts to optimize it always led to breaking of the middle B–N bond to form two BH₂NH₂ molecules. For **10**, the B–N distances range from 1.45 to 1.58 Å; the B–H distances from the bridge are 1.28 and 1.46 Å, and the BHB bond angle is 92.0°. Structure **10** is 9.7 kcal/mol less stable than **4**.

The geometries of the 5,6- and 1,4-isomers of dihydroborazine, (**5**, 1,3,5-triaza-2,4,6-triboracyclohexa-1,3-diene and **6**, 1,3,5-triaza-2,4,6-triboracyclohexa-1,4-diene, in Figure 2, respectively) were optimized. Structure **5** shows a range of B–N distances from 1.39 to 1.64 Å. The latter value is the calculated bond distance between the two adjacent dihydrogenated atoms. Structure **6** has *C*_s symmetry with two unique B–N distances: 1.36 Å between the mono-hydrogenated atoms and 1.57 Å between a mono- and a di-hydrogenated atom. The dipole moments for **5** and **6** are 3.3 and 4.9 (average with the two basis sets) D, respectively, at the B3LYP level.

A planar chain isomer BH₂(NHBH)₂NH₂ (structure **14** in Figure 1) has *C*_s symmetry. The B–N distances for **14** range from 1.41 to 1.45 Å. The planar structure is 3.7 kcal/mol more stable than ring **5**. This result contrasts with the analogous

TABLE 4: Geometry Parameters for Frameworks of $B_xN_xH_y$ Compounds Optimized at the MP2/cc-pVTZ Level^a

compd	BN backbone					BHB bridge	
	r_{BN}	$\angle BNB$	$\angle NBN$	$\angle BNB$	$\angle NBN$	r_{BH}	$\angle BHB$
4	1.6061	87.94	92.05	0.00	0.00		
5	1.6439	109.38	115.73	-45.41	7.19		
	1.3895	123.50	116.11	15.21	6.22		
	1.4831	123.54	103.08	-41.32	58.72		
	1.3886						
1.5345							
6	1.5729	120.80	111.19	2.91	-52.81		
	1.3622	110.47	111.19	52.81	-2.91		
	1.5652	120.80	105.56	-42.48	-42.48		
7	1.6001	116.12	106.15	59.33	-43.84		
	1.5739	116.97	117.53	17.84	-2.43		
	1.6083	130.72	106.29	14.80	-44.68		
	1.5482						
	1.3656						
1.5540							
8a	1.6557	112.97	108.44	180.00			
	1.5410						
	1.6634						
8b	1.6237	116.49	105.77	23.38			
	1.5725						
	1.6162						
9a	1.6459	114.87	108.06	179.28	178.30		
	1.5556	111.10	108.68	178.41			
	1.6528						
	1.5545						
1.6527							
9b	1.6116	119.41	106.89	-50.98	113.79		
	1.5815	118.60	105.70	-47.52			
	1.6051						
	1.5800						
1.6035							
10	1.5845	78.47	115.44	106.68		1.2816	92.00
	1.5425					1.4625	
	1.4540						
11	1.5668	74.64	116.42	-105.59	156.40	1.3295	90.74
	1.5575	114.44	105.11	-179.06		1.3324	
	1.5117						
	1.7011						
	1.5024						
13	1.3774	80.85	159.32	180.00	180.00	1.2879	83.15
	1.4250	122.36	125.63			1.4454	
	1.3370						
	1.5966						
1.3406							
14	1.4132	125.70	121.59	180.00	180.00		
	1.4463	125.25	121.82				
	1.4215						
	1.4432						
	1.4054						

compd	BN backbone				BHB bridge		
	r_{BN}	$\angle BNB$	$\angle NBN$	$\angle BNB$	r_{H-H}	$\angle NH\cdots H$	$\angle BH\cdots H$
12	1.6283	92.31	87.69	0.00	1.99	144.90	88.89

^a Bond lengths (Å) and bond and dihedral angles (degree) are shown in consecutive order of connectivity starting with a boron atom.

hydrocarbon systems (hexatriene is 16 kcal/mol less stable than 1,3-cyclohexadiene) yet is understandable given that the dative π -bond energy in aminoborane (29.9 kcal/mol)⁴⁵ is somewhat stronger than the B–N dative σ bond in ammonia borane (25.9 kcal/mol).⁶

3,4,5,6-tetrahydroborazine (**7** in Figure 2, 1,3,5-triaza-2,4,6-triboracyclohexa-1-ene) has a range of B–N distances from 1.55 to 1.61 Å for bonds involving the di-hydrogenated atoms and a distance of 1.37 Å for the bond between the two mono-hydrogenated atoms. This is consistent with the other calculated geometries where the bonds involving dihydrogenated atoms

are longer than the bonds between the mono-hydrogenated atoms. The dipole moment is predicted to be 3.7 D at the B3LYP level.

Unlike *n*-butane and *n*-hexane which have linear chains, the minimum energy structures of di- and triborazane are coiled because of the intramolecular dihydrogen bonding between the B–H and the N–H bonds.⁴⁶ The molecule $BH_3NH_2BH_2NH_3$ has a linear form ($\angle(B-N-B-N) = 180.0^\circ$, structure **8a** in Figure 1) and a twisted form with a dihedral $\angle(B-N-B-N)$ of 23.4° (structure **8b** in Figure 1). The latter structure is 12.3 kcal/mol more stable at 298 K in terms of the enthalpy. The free energy for the **8a** \rightarrow **8b** process is $\Delta G = -11.3$ kcal/mol. Similarly, the $BH_3(NH_2BH_2)_2NH_3$ twisted structure (**9b** in Figure 1) is 24.6 kcal/mol more stable (enthalpy) than the linear structure (**9a** in Figure 1). The free energy for the **9a** \rightarrow **9b** process is $\Delta G = -21.2$ kcal/mol. Thus, the coiled forms have lower entropies showing that they are more constrained by the head-to-tail hydrogen bonding. The conformational change from linear to twisted **9** is more than twice the exothermicity observed for this structural transition in **8**. The twisted structure, **9b**, has a central dihedral angle, $\angle(B-N-B-N)$, of 113.8° , and the other two dihedral angles are $\sim -50.0^\circ$, whereas the linear structure has all $\angle(B-N-B-N)$ greater than 178.0° . The smallest $H\cdots H$ (head-to-tail) nonbonded distance is ~ 2.00 Å in either of the twisted structures **8b** or **9b**. Thus, these structures are dominated by short electrostatic interactions between the acidic $N-H(\delta^+)$ and the basic $B-H(\delta^-)$ bonds which lead to substantial stabilization of the ring-type chain structures over the linear chains. The short nonbonded $H\cdots H$ interactions are in excellent agreement with the value of 2.02 Å found by a neutron diffraction study of solid NH_3BH_3 by Klooster et al.⁴⁷ and with a theoretical study of the BH_3NH_3 head-to-tail dimer by Cramer and Gladfelter,⁴⁸ who predicted $H\cdots H$ bond distances of 1.99 Å at the MP2/cc-pVDZ level. We can compare the B–N bond distances for **8a** and **8b** with **9a** and **9b**, labeling the backbones as B1–N1–B2–N2 and B1–N1–B2–N2–B3–N3, respectively. For **8**, we find that the linear conformation has B1–N1 and B2–N2 distances of 1.66 Å and a N1–B2 distance of 1.54 Å, whereas the twisted conformation has slightly shorter B1–N1 and B2–N2 distances, 1.62 Å, and a slightly larger N1–B2 distance, 1.57 Å. In a similar way, **9a** has B1–N1, B2–N2, and B3–N3 bond distances of 1.65 Å, a N1–B2 distance of 1.56 Å, and a N2–B3 distance of 1.55 Å, whereas **9b** has shorter B1–N1, B2–N2, and B3–N3 distances, 1.61, 1.61, and 1.60 Å, respectively, and larger N1–B2 and N2–B3 bond distances of 1.58 Å. The changes making the bond distances in the twisted forms more equal are apparently due to the short head-to-tail nonbonded $H\cdots H$ interactions which stabilize the ring chain structures.

Jacquemin et al.⁴⁹ have studied polyaminoboranes ($BH_3(NH_2BH_2)_{n-1}NH_3$) up to 16 BN units long at the PBE0/6-31G-(2d) level for geometries and energies with single point energies at the MP2/6-311G(2d) level. They find a helical and coiled structure to be more stable than the all trans conformation by 5.7 kcal/mol for $n = 2$ and do not report any values for $n = 3$. For larger values of n , their results converge to about 6 kcal/mol. These values are substantially lower than our values consistent with the fact that their structures do not exhibit B–H \cdots N–H bonds. Li et al. have reinvestigated the stability of polyaminoboranes with n up to 5 using DFT methods and examined the effect of branching at nitrogen and boron atoms.⁵⁰ They found coiled structures with intramolecular dihydrogen bonding. Stabilities relative to all trans structures calculated for

TABLE 5: Calculated MP2/cc-pVTZ Vibrational Frequencies and Experimental Values for Borazine

symmetry	expt 1939 ^a	expt 1971 ^b	expt 1967 ^c	this work
e''	288	280	288	282.1
a ₂ ''	415	403	394	395.0
e'	525	518	518	517.8
e''	798	770	798	711.7
a ₂ ''	622	718	719	734.6
a ₁ '	851	845	852	859.3
e''	1070	977	968	930.9
a ₂ ''	1098	913	918	931.3
a ₁ '	938	940	940	949.2
e'	717	1068	990	951.6
a ₂ '	800	782		1052.1
e'	917	1102	1096	1087.3
a ₂ '	1110	1195		1255.1
a ₂ '	1650			1315.9
e'	1466	1394	1406	1402.3
e'	1610	1458	1465	1495.1
e'	2519	2513	2520	2667.2
a ₁ '	2535	(2545)	2535	2676.2
a ₁ '	3450	(3488)	3452	3666.2
e'	3400	3482	3486	3669.3

^a Raman lines and infrared spectrum. Reference 56. ^b ¹¹B Ar matrix. Values in parenthesis from Raman data. Reference 55. ^c Species a₁' and e'' Raman lines, species a₂'' and e' gas-phase infrared spectra. Reference 54.

n = 1 and 2 are very similar to what we find for oligomers **8** and **9**, respectively.

The head-to-tail dimer of BH₃NH₃ (**12** in Figure 1) is 14.0 kcal/mol more stable than two separated molecules. The dimer has C_{2h} symmetry and is characterized by two short nonbonded B–H···H–N bonds of bond length 1.99 Å at each end of the dimer for a total of four short interactions. These distances are again comparable to those found in the neutron diffraction study of solid NH₃BH₃ (2.02 Å)⁴⁷ and from calculations at the MP2/cc-pVDZ (1.99 Å)⁴⁸ and MP2/6-31++G** levels.⁵¹ Morrison and Siddick⁵² calculated the geometry in the solid by using plane wave DFT methods with a gradient corrected functional and obtained a slightly shorter distance of 1.940 Å. Our calculated B–N bonds in the dimer are 0.03 Å shorter than those in the monomer which are 1.65 Å at the MP2/aug-cc-pVTZ level. Klooster et al.⁴⁷ showed in the crystal structure that the ∠N–H···H tends toward linearity (156°), whereas the ∠B–H···H is bent (106°). This is similar to our results where ∠NH···H is 144.9° and is larger than ∠BH···H = 88.9°; our results for the isolated dimer differ from experimental results by more than 10°, especially for the smaller value. These differences come from the fact that our head-to-tail dimer is structurally different from the neutron diffraction structure, although both have B–H···H–N bonds. Our angles are close to the averages or essentially within the ranges obtained for intermolecular dihydrogen bonds obtained by Richardson et al.⁵³ who examined boron nitrogen compounds from the Cambridge Structure Database. They found 26 B–H···H–N bonds with H···H distances of 1.7–2.2 Å (average, 1.96 Å), ∠NH···H bond angles of 117–171° (average, 149°), and ∠BH···H bond angles of 90–171° (average, 120°).

Molecular Frequencies. The calculated and experimental vibrational frequencies of **3** are given in Table 5. The frequencies have been measured and re-analyzed a number of times^{54,55} since the original work of Crawford and Edsall.⁵⁶ The BH and NH stretches are predicted to be too high by about 200 cm⁻¹ as expected because of the difference in the calculated harmonic and anharmonic A–H frequencies. The calculated and experimental gas-phase⁵⁴ values for the remaining modes are in very good overall agreement with the experimental values within 20

TABLE 6: Components of Calculated Atomization Energies^a

molecule	ΔE _{CBS} ^b	ΔE _{ZPE} ^c	ΔE _{CV} ^d	ΔE _{SR} ^e	ΔE _{SO} ^f	ΣD ₀ (0 K)
2a	1545.54	98.87 ^g	5.81	-1.29	-0.09	1451.10
2b	1544.40	98.81 ^g	5.81	-1.29	-0.09	1450.02
3	1218.75	58.08 ^h	5.91	-1.22	-0.09	1165.27
4	1018.50	64.47 ^g	3.83	-0.85	-0.06	957.01
5	1305.10	70.48 ^g	5.79	-1.24	-0.09	1239.08
6	1288.78	69.95 ^g	5.84	-1.23	-0.09	1223.36
7	1341.67	83.90 ^g	5.81	-1.25	-0.09	1262.23
8a	1113.44	75.27 ⁱ	3.81	-0.81	-0.06	1041.12
8b	1126.00	76.01 ⁱ	3.89	-0.82	-0.06	1053.00
9a	1620.78	107.62 ⁱ	5.69	-1.26	-0.09	1517.51
9b	1645.58	108.89 ⁱ	5.84	-1.28	-0.09	1541.16
10	1006.70	62.07 ⁱ	3.93	-0.84	-0.06	947.66
11	1508.46	94.58 ⁱ	5.84	-1.28	-0.09	1418.35
12	1233.81	87.63 ^j	3.94	-0.82	-0.06	1149.25
13	1078.94	52.76 ^k	5.61	-1.14	-0.09	1030.55
14	1307.61	68.23 ^k	5.75	-1.21	-0.09	1243.83

^a Results in kcal/mol. The results are given at the MP2/cc-pVTZ geometry. ^b Extrapolated by using eq 2 with CCSD(T)/aVnZ, where *n* = D, T, and Q. ^c Zero point energies were obtained from the average of MP2/cc-pVTZ and experimental values. ^d Core/valence corrections were obtained by CCSD(T)/cc-pwCVTZ. ^e Scalar relativistic correction is based on a CISD/cc-pVTZ calculation. ^f Values obtained from ref 30. ^g Scale factor of 0.980 obtained from *c*-C₆H₁₂. See text. ^h Scale factor of 0.984 obtained from *c*-C₆H₆. See text. ⁱ Scale factor of 0.965 obtained from the MP2/cc-pVTZ ZPE correction and that obtained from ref 6 for BH₃NH₃. ^j Scale factor of 0.968 obtained from the MP2/aug-cc-pVTZ ZPE correction and that obtained from ref 6 for BH₃NH₃. ^k Scale factor of 0.974 obtained from the MP2/cc-pVTZ ZPE correction and that obtained from ref 6 for BH₂NH₂.

cm⁻¹ except for three modes. The e' mode calculated at 952 cm⁻¹ is less than the assigned experimental value by about 40 cm⁻¹ as is found for the e'' mode calculated at 931 cm⁻¹. The biggest difference between the calculated and the experimental values is for the e'' mode calculated at 712 cm⁻¹ as compared with the experimental value of 798 cm⁻¹, a difference of 86 cm⁻¹. The experimental assignment is based on the observation of a very weak Raman line. The ¹¹B₃N₃H₆ spectra obtained in a matrix⁵⁵ can be compared with our calculated values as well. The agreement between the two sets of experimental values is not as good as one would hope for. We find that the a₂' band calculated at 1255 cm⁻¹ is 60 cm⁻¹ above the experimentally assigned matrix value. The experimentally assigned band at 1068 cm⁻¹ seems to be too high as compared with our calculated value and the other experimental result. These results show the overall quality of the calculated vibrational frequencies, and we expect that there will be comparably good agreement for the other molecules whose vibrational frequencies are given as Supporting Information.

Calculated Heats of Formation. The components for the total atomization energies of the compounds are shown in Table 6. There is a substantial core–valence correction of ~0.95 to 1 kcal/mol per B or N atom just as found in alkanes for the C atoms.¹⁶ⁿ The scalar relativistic correction is about -0.8 kcal/mol for compounds with two B and two N atoms and -1.2 to -1.3 kcal/mol for compounds with three B and three N atoms.

The heats of formation of the molecules are given in Table 7 together with the entropies calculated at the MP2/cc-pVTZ level at 298 K. The only experimental value is that derived for **3** (ΔH_f^o(0 K) = -115.8 ± 3.1 kcal/mol and ΔH_f^o(298 K) = -121.9 ± 3.1 kcal/mol)¹¹ which is more negative than our calculated value at 298 K by 6.4 kcal/mol. This is far outside our usual range of errors for such compounds. The experimental value is based on the heat of combustion of liquid **3** forming solid B(OH)₃ and N₂(g) and on vapor pressure measurements as well as on an assumption of the change in heat capacity for

TABLE 7: Gas-Phase Heats of Formation at 0 and 298 K (kcal/mol) and Entropies at 298 K (cal/(mol·K))

molecule	$\Delta H_f(0\text{ K})$ CCSD(T)	$\Delta H_f(298\text{ K})$ CCSD(T) ^a	$\Delta H_f(0\text{ K})$ G3MP2	$\Delta H_f(298\text{ K})$ G3MP2 ^b	$S^{c,d}$ (298 K)
1	-9.1 ^e	-13.5 ^e	-6.3	-10.6	57.15
2a	-85.3	-96.6	-79.3	-90.2	79.31
				(-98.9)	
2b	-84.3	-95.5	-78.1	-89.1	76.71
				(-98.6)	
3	-109.3	-115.5	-103.2	-109.1	68.73
				(-119.1)	
4	-46.4	-53.6	-41.7	-48.7	67.16
				(-55.2)	
5	-79.8	-87.5	-74.0	-81.5	75.77
6	-64.1	-71.8	-58.5	-65.9	75.61
				(-74.4)	
7	-75.9	-85.3	-70.0	-79.2	78.58
8a	-27.4	-35.3	-21.8	-29.5	77.52
8b	-39.2	-47.6	-33.4	-41.5	74.19
9a	-48.5	-59.9	-40.5	-51.6	97.97
9b	-72.1	-84.3	-63.7	-75.4	87.16
10	-37.2	-43.9	-33.8	-39.9	70.48
11	-52.6	-62.8	-44.6	-54.5	88.79
12	-32.2	-41.3	-26.4	-35.0	83.38 ^f
13	25.4	20.4	31.0	26.6	81.35
14	-84.6	-91.2	-77.8	-84.2	84.11
BH ₂ NH ₂	-15.9 ^e	-18.6 ^e	-14.0	-16.7	55.92
				(-19.7)	

^a Theoretical values at 298 K obtained by the same procedure as in ref 32. ^b G3B3 values in parentheses. ^c MP2/cc-pVTZ values. ^d $S(\text{H}_2) = 31.13\text{ cal}/(\text{mol}\cdot\text{K})$ from reference 11. ^e Reference 6. ^f From MP2/aVTZ calculation.

the liquid to vapor transition being that of benzene. This led to the experimental value with an error limit of $\pm 3\text{ kcal/mol}$. If the heat of vaporization is actually somewhat higher, and considering the combustion error limits to be conservative, then our calculated value is at the upper range of the experimental values.

Condensed phase data for the compounds are included in Table 1. The data for solid **1** is from work by Wolf and co-workers.^{5,10} It is based on the average of results from three different methods. Their $\Delta H_f^\circ[\mathbf{1}(\text{s})]$ is $\sim 6\text{ kcal/mol}$ more positive than an earlier determination by Russian workers (as quoted by T-Raissi⁵⁷) who obtained $-42.5 \pm 1.4\text{ kcal/mol}$. Morrison and Siddick⁵² calculated the sublimation energy at 0 K by using plane wave DFT methods with a gradient corrected functional. Neglecting zero point energy and thermal corrections, their predicted value is $\Delta H_{\text{sub}}^\circ = 18.2\text{ kcal/mol}$ at 0 K. This value is reasonably consistent with the value of $\Delta H_{\text{sub}}^\circ = 21\text{ kcal/mol}$ derived from the ΔH_f of Wolf and co-workers for the solid state and our calculated value for the gas phase. The solid-state value for $\Delta H_f^\circ(\mathbf{2})$ can be estimated from the current gas-phase results and vapor pressure–temperature data of solid **2** measured by Leavers et al.¹³ Extrapolating the vapor pressure data to 298 K provides the standard enthalpy and free energy of sublimation: $\Delta H_{\text{sub}}^\circ = 25 \pm 3$ and $\Delta G_{\text{sub}}^\circ = 7.3 \pm 1.0\text{ kcal/mol}$. This yields a value of $-120.5 \pm 4\text{ kcal/mol}$ for the solid-state value for $\Delta H_f^\circ(\mathbf{2})$. We can also re-evaluate the liquid phase $\Delta H_f^\circ(\mathbf{3})$ by taking our calculated gas-phase value and including the heat of vaporization of $7.1 \pm 0.1\text{ kcal/mol}$ to obtain $\Delta H_f^\circ(\mathbf{3})(\text{liquid})$ of $-122.6 \pm 1.1\text{ kcal/mol}$. By using an estimated heat of melting of $1 \pm 0.5\text{ kcal/mol}$ ($T_{\text{melt}} = -55^\circ\text{C}$), we can then obtain $\Delta H_f^\circ(\mathbf{2})(\text{solid})$ of -123.6 kcal/mol .

The above analysis of the thermodynamics leads us to conclude that production of liquid **3** from solid **2** by loss of H₂ is an approximately thermoneutral process compared with it being 19 kcal/mol exothermic in the gas phase. Production of

solid **2** from solid **1** releases 20 kcal/mol of heat compared with 56 kcal/mol in the gas phase. Driving forces for the condensed-phase reactions are also somewhat less compared with the gas phase. Yet, hydrogen release is still too favorable for the reactions to be practically reversed with hydrogen overpressure: $\Delta G_r^\circ[\mathbf{1}(\text{s}) \leftarrow \mathbf{3}(\text{s})] = 6\text{ kcal/mol}$ of **1**; $\Delta G_r^\circ[\mathbf{2}(\text{s}) \leftarrow \mathbf{3}(\text{l})] = 38\text{ kcal/mol}$. Indeed, Baitalov et al. have reported that thermal release of hydrogen from **1** is unaffected by hydrogen pressure up to 600 bar.⁵⁸ Thus, strategies for regeneration of **1** from spent materials such as **3** must involve chemical steps other than the simple application of hydrogen overpressure.

One common approach to predicting the heats of formation of compounds is to use an approximation to our additive method such as one of the G3-based methods. We used the computationally efficient G3MP2 method.³⁴ We have calculated these values as shown in Table 7. All of the G3MP2 heats of formation are too positive by up to $\sim 6\text{ kcal/mol}$ as compared with our CCSD(T)/CBS values. Overall, the G3MP2 method underestimates the stability of these species. For a few of the compounds, we used the computationally more expensive G3B3 method³³ (as compared with G3MP2). As shown in Table 7, the G3B3 method predicts heats of formation that are too negative as compared with the CCSD(T)/CBS values by up to $3\text{--}4\text{ kcal/mol}$.

We are interested in the heats of formation of even larger compounds for which we cannot use our composite CCSD(T)/CBS approach. DFT is an attractive computational alternative to the more expensive CBS or G3 methods. We have thus used the B3LYP/6-311+G** method to estimate the heats for a variety of dehydrogenation and dehydrocoupling reactions involving molecules with 1–3 BN units. This led to differences in the calculated heats that were too large (see Supporting Information, Table S3). One possible way to improve the DFT predictions is to use an isodesmic reaction approach.^{36,59,60} We first benchmarked the DFT method on the basis of some simple hydrocarbon reactions with well-established heats of formation and then used isodesmic reactions involving BN compounds and hydrocarbons to predict the heats of formation of the BN compounds to understand the accuracy of this approach. Table 8 lists some hydrocarbon dehydrogenation energies at the B3LYP/6-311+G** and G3B3 levels. The G3B3 results reproduce the experimental values but the DFT B3LYP values deviate from the experimental values by as much as 10 kcal/mol for compounds with six C atoms. It is important to note that Curtiss and co-workers showed that the B3LYP method progressively worsened in terms of predicting the heats of formation of linear chain alkanes as the length of the chain increased.⁶¹ Table 9 lists isodesmic reactions that could be used to predict the heats of formation of unknown boron/nitrogen/hydrogen compounds at 298 K. The reaction energies at the B3LYP and G3B3 levels are quite similar in most cases. The agreement with the energies based on experimental heats of formation plus the best calculated heats of formation for the B/N/H compounds for the reactions (10)–(19) are in quite good agreement within $1\text{--}3\text{ kcal/mol}$. This suggests a systematic cancellation of errors such that accurate prediction of reaction energies to within a few kilocalories per mole is achievable with relatively inexpensive DFT methods. Difficulties in predicting dative bond energies to better than $1\text{--}3\text{ kcal/mol}$ with B3LYP are consistent with the observations of Gilbert on substituted amineboranes.⁶² The heats of formation derived from these reactions (10)–(19) are given in Table 10. Compared with best calculated heats of formation, the isodesmic DFT and G3B3

TABLE 8: Reaction Enthalpies for Model Hydrocarbon Reactions Calculated with the B3LYP/6-311+G and G3B3 Methods Compared with Experiment^a**

number	reaction	B3LYP	G3B3	expt ^b
3	CH ₃ CH ₃ → CH ₂ =CH ₂ + H ₂	31.9	32.0	32.6
4	2CH ₃ CH ₃ → <i>c</i> -C ₄ H ₈ + 2H ₂	51.0	46.3	46.7
5	2CH ₃ CH ₃ → CH ₃ CH ₂ CH ₂ CH ₃ + H ₂	13.8	9.8	10.1
6	3CH ₃ CH ₃ → CH ₃ CH ₂ CH ₂ CH ₂ CH ₂ CH ₃ + 2H ₂	27.8	19.4	20.2
7	3CH ₃ CH ₃ → <i>c</i> -C ₆ H ₁₂ + 3H ₂	41.5	30.0	30.7
8	<i>c</i> -C ₆ H ₁₂ → <i>c</i> -C ₆ H ₆ + 3H ₂	40.3	48.1	49.3
9	<i>c</i> -1,4-C ₆ H ₈ → <i>c</i> -C ₆ H ₆ + H ₂	-10.1	-6.3	-5.0

^a Units are kcal/mol, 298 K. ^b Reference 11b.

TABLE 9: Isodesmic Reaction Enthalpies Calculated with B3LYP/6-311+G and G3B3 Methods^a**

number	reaction	DFT	G3B3	expt ^b
10	BH ₃ NH ₃ + CH ₂ =CH ₂ → BH ₂ =NH ₂ + CH ₃ CH ₃	-39.9	-38.2	-37.7
11	2BH ₃ NH ₃ + <i>c</i> -C ₄ H ₈ → <i>c</i> -B ₂ N ₂ H ₈ + 2CH ₃ CH ₃	-74.7	-74.5	-73.3
12	2BH ₃ NH ₃ + <i>n</i> -C ₄ H ₁₀ → BH ₃ NH ₂ BH ₂ NH ₃ + 2C ₂ H ₆	-29.9	-30.5	-30.6
13	3BH ₃ NH ₃ + <i>c</i> -C ₆ H ₁₂ → <i>c</i> -B ₃ N ₃ H ₁₂ + 3CH ₃ CH ₃	-88.7	-88.1	-86.8
14	3BH ₃ NH ₃ + <i>n</i> -C ₆ H ₁₄ → BH ₃ (NH ₂ BH ₂) ₂ NH ₃ + 3C ₂ H ₆	-61.9		-64.0
15	3BH ₃ NH ₃ + <i>c</i> -C ₆ H ₆ → <i>c</i> -B ₃ N ₃ H ₆ + 3CH ₃ CH ₃	-156.8	-156.7	-154.9
16	<i>c</i> -B ₃ N ₃ H ₆ + <i>c</i> -C ₆ H ₁₂ → <i>c</i> -B ₃ N ₃ H ₁₂ + <i>c</i> -C ₆ H ₆	68.0	68.6	68.2
17	<i>c</i> -B ₃ N ₃ H ₆ + <i>c</i> -C ₆ H ₁₀ → <i>c</i> -B ₃ N ₃ H ₁₀ + <i>c</i> -C ₆ H ₆	49.6		51.1
18	<i>c</i> -B ₃ N ₃ H ₆ + <i>c</i> -5,6-C ₆ H ₈ → <i>c</i> -5,6-B ₃ N ₃ H ₈ + <i>c</i> -C ₆ H ₆	20.5		22.8
19	<i>c</i> -B ₃ N ₃ H ₆ + <i>c</i> -1,4-C ₆ H ₈ → <i>c</i> -1,4-B ₃ N ₃ H ₈ + <i>c</i> -C ₆ H ₆	36.5	38.5	39.5

^a Units are kcal/mol, referenced to the compounds in the gas-phase standard state, 1 atm, 298 K. Structures for *c*-C₆H₁₂ and *c*-B₃N₃H₁₂ are the chair conformations. ^b Uses experimental ΔH_f° for hydrocarbons and CCSD(T) ΔH_f° for B–N–H compounds (Table 7).

TABLE 10: Calculated ΔH_f° at the B3LYP/6-311+G and G3B3 Levels from Isodesmic Reaction Energies (Table 9)^a**

molecule	isodesmic/DFT	isodesmic/G3B3	CCSD(T)/CBS
BH ₂ NH ₂	-20.8	-19.1	-18.6
4	-55	-54.8	-53.6
8b	-46.8	-47.4	-47.6
3	-117.3	-117.2	-115.5
5	-91.8		-87.5
6	-75.8	-73.7	-71.8
7	-88.6		-85.3
2b (chair)	-98.5	-97.9	-95.5
2a (twist boat)	-98.9		-96.6
9b	-82.2		-84.3

^a Uses experimental ΔH_f° of the hydrocarbons^{11b} and ΔH_f° (BH₃NH₃) = -13.5 kcal/mol.⁶

values tend to overestimate the stability of the BN containing compounds by 2 ± 2 kcal/mol. Two exceptions are **8b** and **9b**.

Entropies. The calculated entropies are given in Table 7. Calculated entropies of C₂ and cyclic hydrocarbons are in good agreement with measured values. However, the harmonic oscillator approximation may introduce errors when internal rotors are present. For example, calculated entropies of the normal alkanes ($n > 2$) deviate from experimental entropies by an amount that increases monotonically with the carbon number.⁶³ Because of the strong hydrogen bonds in the “linear” structures, there may be fewer rotamers than in the hydrocarbon case which will reduce the errors due to using the harmonic, rigid rotor approximation.

Reaction Energies. We can use the calculated heats of formation to predict the energies of a variety of reactions for the release of H₂ as well as for condensation and rearrangement reactions as shown in Table 11. We first continue our discussion of the energetics of reaction 1. The enthalpies for the gas-phase reactions **1** → **2** → **3** are quite negative, -56.1 kcal/mol for the first step and -18.9 kcal/mol for the second step. The corresponding condensed phase reaction energies are -10.7 kcal/mol for the first step (solid to solid) and -2.1 kcal/mol for the second step (solid to liquid). Thus, the intermolecular forces in the solid state are quite strong for BH₃NH₃, and they

get weaker as **1** goes to form **2** and **3**. The energy to form gas-phase molecules per BN unit is 21, 8, and 2 kcal/mol for **1**, **2**, and **3**, respectively. The driving forces for these reactions are the conversion of the dative σ bonds in BH₃NH₃ into stronger delocalized dative σ bonds in *c*-B₃N₃H₁₂ into very strong B–N σ bonds in *c*-B₃N₃H₆.⁴⁵

Reactions 40 to 47 show some interesting trends in how **3** is formed from **2**. First, reaction 47 shows that loss of H₂ from *c*-B₃N₃H₁₂ to form *c*-B₃N₃H₁₀ is endothermic with $\Delta H = 11.4$ kcal/mol; ΔG is lowered to 2.4 kcal/mol because of the production of the H₂ molecule. The 5,6-isomer of *c*-B₃N₃H₈ is substantially more stable than the 1,4-isomer by 15.7 kcal/mol at 298 K. The loss of H₂ from *c*-B₃N₃H₁₀ to form 5,6-*c*-B₃N₃H₈ (reaction 43) is slightly exothermic with $\Delta H = -2.1$ kcal/mol and $\Delta G = -10.6$ kcal/mol. The loss of the final H₂ from 5,6-*c*-B₃N₃H₈ to form *c*-B₃N₃H₆ (reaction 40) is substantially exothermic by -27.9 kcal/mol, showing the additional stability of *c*-B₃N₃H₆. We can make an estimate of the “resonance energy” in *c*-B₃N₃H₆ by accounting for the -2.1 kcal/mol from reaction 43 which allows us to estimate the resonance energy as 26 kcal/mol, falling between the values of 20 and 30–36 kcal/mol commonly used for benzene.^{64–66} Han et al. predicted the reaction energy of reaction 40 to be -25.6 kcal/mol and that of reaction 41 to be -41.5 kcal/mol at the B3LYP/6-311G** level in reasonable agreement with our results.⁶⁷ Zhang et al. have studied the hydrogenation energies of the BN compound isoelectronic to barrelene at the B3LYP and G3MP2B3 levels to form the fully hydrogenated compounds.⁶⁸ They predict the dehydrogenation of the fully hydrogenated BN barrelene derivative to be endothermic by 2.8 kcal/mol at 298 K. The second step is slightly exothermic at 3.2 kcal/mol, and the third step is substantially exothermic at 16.2 kcal/mol. This is similar to the ordering of the energies that we found from **2** progressing through **5** and **7** to form **3**. The energy differences in hydrogenation of barrelene were attributed to strain energies, but on the basis of our results, it is more likely due to differences in the B–N bond energies.

Formation of the head-to-tail dimer (reaction 50) is substantially exothermic by 14.3 kcal/mol at 298 K. On the basis of

TABLE 11: Enthalpies (kcal/mol), Entropies (cal/(mol·K)), and Free Energies (kcal/mol) of Reactions

number	reaction	ΔH^a (0 K)	ΔH^a (298 K)	ΔS^c (298 K)	ΔG (298 K)
20	$2\text{BH}_3\text{NH}_3 \rightarrow c\text{-B}_2\text{N}_2\text{H}_8 + 2\text{H}_2$	-28.1	-26.4	15.12	-30.9
21	$3\text{BH}_3\text{NH}_3 \rightarrow c\text{-B}_3\text{N}_3\text{H}_{12}$ (twist-boat) + 3H_2	-57.9	-55.9	1.25	-56.2
22	$c\text{-B}_3\text{N}_3\text{H}_{12}$ (twist-boat) $\rightarrow c\text{-B}_3\text{N}_3\text{H}_6 + 3\text{H}_2$	-23.9	-18.7	82.81	-43.3
23	$2\text{BH}_3\text{NH}_3 \rightarrow \text{BH}_3\text{NH}_2\text{BH}_2\text{NH}_3$ (twist) + H_2	-21.0	-20.5	-8.98	-17.8
24	$3\text{BH}_3\text{NH}_3 \rightarrow \text{BH}_3(\text{NH}_2\text{BH}_2)_2\text{NH}_3$ (twist) + 2H_2	-44.7	-43.6	-22.03	-37.1
25	$(\text{BH}_2\text{NH}_2)_3 \rightarrow c\text{-B}_3\text{N}_3\text{H}_{12}$ (twist-boat)	-32.7	-33.8	-9.48	-31.0
26	$(\text{BHNH})_3 \rightarrow c\text{-B}_3\text{N}_3\text{H}_6$	-134.7	-135.9	-12.62	-132.1
27	$\text{BH}_2(\text{NHBH})_2\text{NH}_2 \rightarrow c\text{-B}_3\text{N}_3\text{H}_6 + \text{H}_2$	-24.7	-24.2	15.75	-28.9
28	$\text{BH}_3(\text{NH}_2\text{BH}_2)_2\text{NH}_3$ (twist) $\rightarrow c\text{-B}_3\text{N}_3\text{H}_{12}$ (twist-boat) + H_2	-13.2	-12.2	23.28	-19.2
29	$c\text{-B}_3\text{N}_3\text{H}_{12}$ (twist-boat) $\rightarrow \text{BH}_2(\text{NHBH})_2\text{NH}_2 + 2\text{H}_2$	0.8	5.6	67.06	-14.4
30	$\text{BH}_2\text{NH}_2\text{BH}_2\text{NH}_2$ (bridge) $\rightarrow c\text{-B}_2\text{N}_2\text{H}_8$	-9.2	-9.7	-3.32	-8.7
31	$\text{BH}_3\text{NH}_2\text{BH}_2\text{NH}_3$ (twist) $\rightarrow c\text{-B}_2\text{N}_2\text{H}_8 + \text{H}_2$	-7.2	-5.9	24.10	-13.1
32	$2\text{BH}_2\text{NH}_2 \rightarrow c\text{-B}_2\text{N}_2\text{H}_8$	-14.6	-16.4	-44.68	-3.1
33	$3\text{BH}_2\text{NH}_2 \rightarrow c\text{-B}_3\text{N}_3\text{H}_6 + 3\text{H}_2$	-61.5	-59.5	-5.64	-57.8
34	$3\text{BH}_2\text{NH}_2 \rightarrow c\text{-B}_3\text{N}_3\text{H}_{12}$ (twist-boat)	-37.6	-40.8	-88.45	-14.4
35	$3\text{BH}_2\text{NH}_2 \rightarrow \text{BH}_2(\text{NHBH})_2\text{NH}_2 + 2\text{H}_2$	-36.8	-35.2	-21.39	-28.9
36	$3\text{BH}_2\text{NH}_2 \rightarrow c\text{-5,6-B}_3\text{N}_3\text{H}_8 + 2\text{H}_2$	-32.0	-31.5	-29.73	-22.7
37	$\text{BH}_3\text{NH}_2\text{BH}_2\text{NH}_3$ (twist) $\rightarrow 2\text{BH}_2\text{NH}_2 + \text{H}_2$	7.4	10.5	68.78	-10.0
38	$\text{BH}_3(\text{NH}_2\text{BH}_2)_2\text{NH}_3$ (twist) $\rightarrow 3\text{BH}_2\text{NH}_2 + \text{H}_2$	24.4	28.6	111.73	-4.7
39	$\text{BH}_3\text{NH}_3 \rightarrow \text{BH}_2\text{NH}_2 + \text{H}_2$	-6.8	-5.0	29.90	-13.9
40	$c\text{-5,6-B}_3\text{N}_3\text{H}_8 \rightarrow c\text{-B}_3\text{N}_3\text{H}_6 + \text{H}_2$	-29.5	-27.9	24.09	-35.1
41	$c\text{-1,4-B}_3\text{N}_3\text{H}_8 \rightarrow c\text{-B}_3\text{N}_3\text{H}_6 + \text{H}_2$	-45.2	-43.6	24.25	-50.9
42	$c\text{-B}_3\text{N}_3\text{H}_{10} \rightarrow c\text{-B}_3\text{N}_3\text{H}_6 + 2\text{H}_2$	-33.3	-30.0	52.54	-45.7
43	$c\text{-B}_3\text{N}_3\text{H}_{10} \rightarrow c\text{-5,6-B}_3\text{N}_3\text{H}_8 + \text{H}_2$	-3.9	-2.1	28.45	-10.6
44	$c\text{-B}_3\text{N}_3\text{H}_{10} \rightarrow c\text{-1,4-B}_3\text{N}_3\text{H}_8 + \text{H}_2$	11.8	13.6	28.29	5.1
45	$c\text{-B}_3\text{N}_3\text{H}_{12}$ (twist-boat) $\rightarrow c\text{-5,6-B}_3\text{N}_3\text{H}_8 + 2\text{H}_2$	5.6	9.3	58.72	-8.2
46	$c\text{-B}_3\text{N}_3\text{H}_{12}$ (twist-boat) $\rightarrow c\text{-1,4-B}_3\text{N}_3\text{H}_8 + 2\text{H}_2$	21.3	25.0	58.56	7.5
47	$c\text{-B}_3\text{N}_3\text{H}_{12}$ (twist-boat) $\rightarrow c\text{-B}_3\text{N}_3\text{H}_{10} + \text{H}_2$	9.4	11.4	30.27	2.4
48	$(\text{BH}_3\text{NH}_3)_2$ (dimer) $\rightarrow c\text{-B}_2\text{N}_2\text{H}_8 + 2\text{H}_2$	-14.1	-12.1	46.04	-25.9
49	$(\text{BH}_3\text{NH}_3)_2$ (dimer) $\rightarrow \text{BH}_3\text{NH}_2\text{BH}_2\text{NH}_3$ (twist) + H_2	-7.0	-6.2	21.94	-12.8
50	$2\text{BH}_3\text{NH}_3 \rightarrow (\text{BH}_3\text{NH}_3)_2$ (dimer)	-14.0	-14.3	-30.92	-5.1
51	$\text{BH}_3\text{NH}_2\text{BH}_2\text{NH}_3 \rightarrow \text{BH}_3\text{NH}_2\text{BH}_2\text{NH}_3$ (twist)	-11.8	-12.3	-3.33	-11.3
52	$\text{BH}_3(\text{NH}_2\text{BH}_2)_2\text{NH}_3 \rightarrow \text{BH}_3(\text{NH}_2\text{BH}_2)_2\text{NH}_3$ (twist)	-23.6	-24.4	-10.81	-21.2
53	$c\text{-5,6-B}_3\text{N}_3\text{H}_8 \rightarrow \text{BH}_2(\text{NHBH})_2\text{NH}_2$	-4.8	-3.7	8.3	-6.2

^a $\Delta H_{f,0\text{K}}(\text{BH}_3\text{NH}_3) = -9.1$ kcal/mol and $\Delta H_{f,298\text{K}}(\text{BH}_3\text{NH}_3) = -13.5$ kcal/mol, ref 6. We used for this level $\Delta H_{f,0\text{K}}(\text{H}_2) = 0.03$ kcal/mol and $\Delta H_{f,298\text{K}}(\text{H}_2) = 0.08$ kcal/mol. ^b At the G3MP2 level: $\Delta H_{f,0\text{K}}(\text{H}_2) = -1.2$ kcal/mol and $\Delta H_{f,298\text{K}}(\text{H}_2) = -1.1$ kcal/mol. ^c Entropy of reaction was calculated from MP2/cc-pVTZ values, where $S(\text{BH}_3\text{NH}_3) = 57.15$ cal/(mol·K) and $S(\text{H}_2) = 31.10$ cal/(mol·K).

the presence of four H···H nonbonded interactions, we can estimate the H···H nonbonded interaction energy to be 3.6 kcal/mol at 298 K and 3.5 kcal/mol at 0 K with ZPE corrections. At the electronic energy level, the H···H bond energy is 4.0 kcal/mol. This is substantially larger than the value of 2.8 kcal/mol obtained by a similar procedure at the MP2/6-31++G** level at 0 K with ZPE corrections and 3.3 kcal/mol without corrections.⁵¹ On the basis of a DFT solid-state calculation starting from the crystal structure orientation, a hydrogen bond energy value of 3.0 kcal/mol at 0 K was obtained with no ZPE correction. We note that the crystal structure does not have head-to-tail dimers. Using the fact that there are six effective H···H nonbonded interactions per molecule in the solid state and assuming that it is only these interactions which contribute to the stability of the solid state, we obtain an estimate of the cohesive energy of 21.6 kcal/mol which is in excellent agreement with the value of 21 kcal/mol derived from our gas-phase monomer energy and the solid state ΔH_f° obtained by Wolf and co-workers.⁵ Thus, the stability of the solid-state phase of BH_3NH_3 is driven almost completely by the formation of H···H hydrogen bonds. The strength of the H···H bond can be compared to that of the OH···O bond in the H_2O dimer which is 5.0 kcal/mol with no ZPE correction.⁶⁹ Thus, the H···H bond is about 1 kcal/mol weaker than the hydrogen bond in the H_2O dimer and is a medium strength H bond. We note that, at 298 K, the entropy effects are largely due to the formation of a free particle and that the value of ΔG to form the dimer is only -1.5 kcal/mol.

The reverse of reaction 25 provides the B(H₂)–N(H₂) bond strength in **2a**, and this value is 32.7 kcal/mol at 0 K, slightly

higher than the value of the B–N bond strength in **1** of 25.9 kcal/mol.⁶ We note that compound **11** has bridging H and NH₂ groups. The B(H₂)–N(H₂) bond energy in **5** to form **14** (reaction 53) is actually negative with a value of -4.8 kcal/mol. The B(H₂)–N(H₂) bond energy in **4** leading to the formation of **10** (reverse of reaction 30) is only 9.2 kcal/mol showing evidence of about 24 kcal/mol of ring strain on the basis of reaction 25. The reverse of reaction 26 is the B(H)–N(H) bond energy in **3** and is 134.7 kcal/mol as compared with the B–N bond energy in BH_2NH_2 of 139.7 kcal/mol. There is no apparent resonance stabilization in **3** on the basis of this comparison. The components of the B–N bond in BH_2NH_2 (strong σ bond and weak π -donor bond) have been discussed in detail.⁴⁵

One step on the way to forming **2** from **1** is the reaction of two molecules of **1** to form **4** with the release of two H_2 (reaction 20). This reaction is substantially exothermic with $\Delta H = -22.8$ kcal/mol at 298 K and $\Delta G = -31.1$ kcal/mol. Thus, depending on the kinetics, dimerization of **1** could lead to a four-member ring with loss of H_2 . The reaction of $(\text{BH}_3\text{NH}_3)_2$ or **12** to form **4** and two molecules of H_2 is still exothermic by 12.1 kcal/mol. Reaction of **4** with BH_3NH_3 and loss of H_2 to form **2** is 29.5 kcal/mol exothermic. We also note that dimerization of BH_2NH_2 to form **4** is exothermic by 16.4 kcal/mol (reaction 32).

As discussed above, there is also the possibility that the polymerization of BH_3NH_3 could lead to chains. Such chains could also be intermediates on the way to forming ring compounds. The first such reaction is the dimerization of BH_3NH_3 to form **8b** releasing H_2 (reaction 23) which is exothermic by 16.9 kcal/mol at 298 K. Elimination of a second H_2 to form

the ring compound **4** (reaction 31) is exothermic by only 5.9 kcal/mol at 298 K. Addition of BH_3NH_3 to **8b** followed by elimination of H_2 to form **9b** is exothermic by 21.3 kcal/mol. The final elimination of H_2 from **9b** to form **2** (reaction 28) is exothermic by 12.2 kcal/mol at 298 K and has $\Delta G = -19.2$ kcal/mol because of the formation of the H_2 molecule. Thus, these chains can certainly serve as intermediate species in the formation of the ring compounds. The chains are stable to the loss of H_2 and the formation of BH_2NH_2 . The twisted molecular trimer **9b** can eliminate three H_2 and form **14** in an exothermic fashion with $\Delta H = -6.9$ kcal/mol.

Summary

This work provides the first complete analysis of the thermodynamic cycle of hydrogen release and uptake for the chemical hydrogen storage compounds linked to borazane in the gas and condensed phases. Accurate gas-phase heats of formation were calculated by using ab initio molecular orbital theory at the CCSD(T)/CBS level with additional corrections for 16 $\text{B}_x\text{N}_x\text{H}_y$ compounds with $x = 2, 3$ and $y \geq 2x$. These results were used to benchmark the G3MP2 and G3B3 methods as well as DFT with the hybrid B3LYP exchange-correlation functional. The G3MP2 and G3B3 heats of formation differ by up to ~ 6 kcal/mol as compared with CCSD(T)/CBS values. DFT at the B3LYP/6-311+G** level was able to predict isodesmic reaction energies to within a few kcal/mol compared to the CCSD(T)/CBS method so isodesmic reaction energies calculated at this level of DFT can be used to estimate heats of formation of larger $\text{B}_x\text{N}_x\text{H}_y$ compounds which are less accessible by the higher level G3 and CCSD(T) methods. Enthalpies, entropies, and free energies were calculated for many dehydrocoupling and dehydrogenation reactions that convert BNH_6 to alicyclic and cyclic oligomers and $\text{H}_2(\text{g})$. Generally, the reactions are highly exothermic, and exergonic as well, due to the release of 1 or more equivalents of $\text{H}_2(\text{g})$. For $c\text{-B}_3\text{N}_3\text{H}_{12}$ and $c\text{-B}_3\text{N}_3\text{H}_6$, the available experimental data for sublimation and vaporization lead to estimates of their condensed phase 298 K heats of formation as $\Delta H_f^\circ[c\text{-B}_3\text{N}_3\text{H}_{12}(\text{s})] = -124$ kcal/mol and $\Delta H_f^\circ[c\text{-B}_3\text{N}_3\text{H}_6(\text{l})] = -123$ kcal/mol. The reaction thermochemistry for the dehydrocoupling of $\text{BNH}_6(\text{s})$ to $c\text{-B}_3\text{N}_3\text{H}_{12}(\text{s})$ and the dehydrogenation of $c\text{-B}_3\text{N}_3\text{H}_{12}(\text{s})$ to $c\text{-B}_3\text{N}_3\text{H}_6(\text{l})$ are much less exothermic compared with the gas-phase reactions due to intermolecular forces which decrease in the order $\text{BNH}_6 > c\text{-B}_3\text{N}_3\text{H}_{12} > c\text{-B}_3\text{N}_3\text{H}_6$. The calculation of the energy of the intermolecular forces due to the interaction of the acidic $\text{N}-\text{H}(\delta^+)$ and basic $\text{B}-\text{H}(\delta^-)$ bonds to form $\text{H}\cdots\text{H}$ nonbonded interactions in the dimer of BH_3NH_3 leads to a value of 4.0 kcal/mol at the electronic energy level which is about 1 kcal/mol less than the value for the $\text{O}-\text{H}\cdots\text{O}$ hydrogen bond in the water dimer. This value is consistent with the structure of solid BH_3NH_3 and its cohesive energy. The condensed phase reaction free energies are less negative compared with the gas-phase reactions, but still too unfavorable for BNH_6 to be regenerated with H_2 from either $c\text{-B}_3\text{N}_3\text{H}_{12}$ or $c\text{-B}_3\text{N}_3\text{H}_6$ by just an overpressure of H_2 .

Acknowledgment. Support for this work at both the University of Alabama and Pacific Northwest National Laboratory was provided through the DOE Center of Excellence for Chemical Hydrogen Storage of the Hydrogen Program at the U.S. Department of Energy. D.A.D. thanks the Robert Ramsay Fund of the University of Alabama. NWChem Version 4.7, as developed and distributed by Pacific Northwest National Laboratory, P. O. Box 999, Richland, Washington 99352,

U.S.A., and funded by the U.S. Department of Energy, was used to obtain some of these results. Part of this research was performed in the William R. Wiley Environmental Molecular Sciences Laboratory (EMSL) at the Pacific Northwest National Laboratory (PNNL) using the Molecular Sciences Computing Facility. The EMSL is a national user facility funded by the Office of Biological and Environmental Research in the U.S. Department of Energy. PNNL is a multiprogram national laboratory operated by Battelle Memorial Institute for the U.S. Department of Energy.

Supporting Information Available: CCSD(T) energies (E_h); calculated MP2/cc-pVTZ frequencies; enthalpies (kcal/mol) as a function of method; entropies (cal/(mol·K)) and free energies (kcal/mol) of reactions 20–52; and Cartesian coordinates for $\text{B}_x\text{N}_x\text{H}_y$ compounds. This material is available free of charge via the Internet at <http://pubs.acs.org>.

References and Notes

- (1) (a) *Basic Energy Needs for the Hydrogen Economy*; Dressalhaus, M., Crabtree, G., Buchanan, M., Eds.; Baic Energy Sciences, Office of Science, U.S. Department of Energy: Washington, DC, 2003. (b) Maelund, A. J.; Hauback, B. C. In *Advanced Materials for the Energy Conversion II*; Chandra, D., Bautista, R. G., Schlapbach, L., Eds.; The Minerals, Metals and Materials Society: Warrendale, PA, 2004.
- (2) Parry, R. W.; Schultz, D. R.; Girardot, P. R. *J. Am. Chem. Soc.* **1958**, *80*, 1.
- (3) Sorokin, V. P.; Vesnina, B. I.; Klimova, N. S. *Russ. J. Inorg. Chem.* **1963**, *8*, 32.
- (4) (a) Geanangel, R. A.; Wendlandt, W. W. *Thermochim. Acta* **1985**, *86*, 375. (b) Sit, V.; Geanangel, R. A.; Wendlandt, W. W. *Thermochim. Acta* **1987**, *113*, 379. (c) Wang, J. S.; Geanangel, R. A. *Inorg. Chim. Acta* **1988**, *148*, 185.
- (5) (a) Wolf, G.; van Miltenburg, R. A.; Wolf, U. *Thermochim. Acta* **1998**, *317*, 111. (b) Wolf, G.; Baumann, J.; Baitalov, F.; Hoffmann, F. P. *Thermochim. Acta* **2000**, *343*, 19. (c) Baitalov, F.; Baumann, J.; Wolf, G.; Jaenicke-Rlobler, K.; Leitner, G. *Thermochim. Acta* **2002**, *391*, 159.
- (6) Dixon, D. A.; Gutowski, M. J. *Phys. Chem. A* **2005**, *109*, 5129.
- (7) Gutowska, A.; Li, L.; Shin, Y.; Wang, C.; Li, S.; Linehan, J.; Smith, R. S.; Kay, B.; Schmid, B.; Shaw, W.; Gutowski, M.; Autrey, T. *Angew. Chem., Int. Ed.* **2005**, *44*, 2.
- (8) (a) Li, Q. S.; Zhang, J.; Zhang, S. *Chem. Phys. Lett.* **2005**, *404*, 100. (b) Zhang, J.; Zhang, S.; Li, Q. S. *J. Mol. Struct.: THEOCHEM* **2005**, *717*, 33.
- (9) Jaska, C. A.; Temple, K.; Lough, A. J.; Manners, I. *J. Am. Chem. Soc.* **2003**, *125*, 9424.
- (10) (a) Baumann, J. Dissertation, TU Bergakademie Freiberg, Germany, 2003. (b) Wolf, G. In *W. E.-Heraeus-Seminar on Hydrogen Storage with Novel Nanomaterials*; Bad Honnef, Germany, October 23–27, 2005 (http://www.h-workshop.uni-konstanz.de/pdf/Wolf_Gert.pdf).
- (11) Chase, M. W., Jr.; NIST-JANAF Tables, 4th ed., *J. Phys. Chem. Ref. Data*, Mono. 9, Suppl. 1, 1998. See also Linstrom, P. J.; Mallard, W. G. Eds. *NIST Chemistry WebBook*, NIST Standard Reference Database Number 69, June 2005, National Institute of Standards and Technology, Gaithersburg MD, 20899 (<http://webbook.nist.gov/chemistry/>).
- (12) *Lange's Handbook of Chemistry*, 13th ed.; Dean, J. A., Ed.; McGraw-Hill: New York, 1985; Chapter 9, p 11.
- (13) Leavers, D. R.; Long, J. R.; Shore, S. G.; Taylor, W. J. *J. Chem. Soc. A* **1969**, 1580.
- (14) Stephens, F. H.; Baker, R. T.; Matus, M. H.; Grant, D. J.; Dixon, D. A. *Angew. Chem., Int. Ed.* **2007**, *46*, 746.
- (15) (a) Purvis, G. D., III; Bartlett, R. J. *J. Chem. Phys.* **1982**, *76*, 1910. (b) Raghavachari, K.; Trucks, G. W.; Pople, J. A.; Head-Gordon, M. *Chem. Phys. Lett.* **1989**, *157*, 479. (c) Watts, J. D.; Gauss, J.; Bartlett, R. J. *J. Chem. Phys.* **1993**, *98*, 8718.
- (16) (a) Peterson, K. A.; Xantheas, S. S.; Dixon, D. A.; Dunning, T. H., Jr. *J. Phys. Chem. A* **1998**, *102*, 2449. (b) Feller, D.; Peterson, K. A. *J. Chem. Phys.* **1998**, *108*, 154. (c) Dixon, D. A.; Feller, D. *J. Phys. Chem. A* **1998**, *102*, 8209. (d) Feller, D.; Peterson, K. A. *J. Chem. Phys.* **1999**, *110*, 8384. (e) Feller, D.; Dixon, D. A. *J. Phys. Chem. A* **1999**, *103*, 6413. (f) Feller, D. *J. Chem. Phys.* **1999**, *111*, 4373. (g) Feller, D.; Dixon, D. A. *J. Phys. Chem. A* **2000**, *104*, 3048. (h) Feller, D.; Sordo, J. A. *J. Chem. Phys.* **2000**, *113*, 485. (i) Feller, D.; Dixon, D. A. *J. Chem. Phys.* **2001**, *115*, 3484. (j) Dixon, D. A.; Feller, D.; Sandrone, G. *J. Phys. Chem. A* **1999**, *103*, 4744. (k) Ruscic, B.; Wagner, A. F.; Harding, L. B.; Asher, R. L.; Feller, D.; Dixon, D. A.; Peterson, K. A.; Song, Y.; Qian, X.; Ng, C.; Liu, J.; Chen, W.; Schwenke, D. W. *J. Phys. Chem. A* **2002**, *106*, 2727. (l) Feller,

- D.; Dixon, D. A.; Peterson, K. A. *J. Phys. Chem. A* **1998**, *102*, 7053. (m) Dixon, D. A.; Feller, D.; Peterson, K. A. *J. Chem. Phys.* **2001**, *115*, 2576. (n) Pollack, L.; Windus, T. L.; de Jong, W. A.; Dixon, D. A. *J. Phys. Chem. A* **2005**, *109*, 6934. (o) Dixon, D. A.; Gutowski, M. *J. Phys. Chem. A* **2005**, *109*, 5129. (p) Dixon, D. A.; Arduengo, A. J., Jr. *J. Phys. Chem. A* **2006**, *110*, 1968. (q) Grant, D. J.; Dixon, D. A. *J. Phys. Chem. A* **2005**, *109*, 10138.
- (17) Frisch, M. J.; Trucks, G. W.; Schlegel, H. B.; Scuseria, G. E.; Robb, M. A.; Cheeseman, J. R.; Montgomery, J. A., Jr.; Vreven, T.; Kudin, K. N.; Burant, J. C.; Millam, J. M.; Iyengar, S. S.; Tomasi, J.; Barone, V.; Mennucci, B.; Cossi, M.; Scalmani, G.; Rega, N.; Petersson, G. A.; Nakatsuji, H.; Hada, M.; Ehara, M.; Toyota, K.; Fukuda, R.; Hasegawa, J.; Ishida, M.; Nakajima, T.; Honda, Y.; Kitao, O.; Nakai, H.; Klene, M.; Li, X.; Knox, J. E.; Hratchian, H. P.; Cross, J. B.; Bakken, V.; Adamo, C.; Jaramillo, J.; Gomperts, R.; Stratmann, R. E.; Yazyev, O.; Austin, A. J.; Cammi, R.; Pomelli, C.; Ochterski, J. W.; Ayala, P. Y.; Morokuma, K.; Voth, G. A.; Salvador, P.; Dannenberg, J. J.; Zakrzewski, V. G.; Dapprich, S.; Daniels, A. D.; Strain, M. C.; Farkas, O.; Malick, D. K.; Rabuck, A. D.; Raghavachari, K.; Foresman, J. B.; Ortiz, J. V.; Cui, Q.; Baboul, A. G.; Clifford, S.; Cioslowski, J.; Stefanov, B. B.; Liu, G.; Liashenko, A.; Piskorz, P.; Komaromi, I.; Martin, R. L.; Fox, D. J.; Keith, T.; Al-Laham, M. A.; Peng, C. Y.; Nanayakkara, A.; Challacombe, M.; Gill, P. M. W.; Johnson, B.; Chen, W.; Wong, M. W.; Gonzalez, C.; Pople, J. A. *Gaussian 03*, revision C.01; Gaussian, Inc.: Wallingford, CT, 2004.
- (18) Werner, H.-J.; Knowles, P. J.; Amos, R. D.; Bernhardsson, A.; Berning, A.; Celani, P.; Cooper, D. L.; Deegan, M. J. O.; Dobbyn, A. J.; Eckert, F.; Hampel, C.; Hetzer, G.; Knowles, P. J.; Korona, T.; Lindh, R.; Lloyd, A. W.; McNicholas, S. J.; Manby, F. R.; Meyer, W.; Mura, M. E.; Nicklass, A.; Palmieri, P.; Pitzer, R.; Rauhut, G.; Schütz, M.; Schumann, U.; Stoll, H.; Stone, A. J.; Tarroni, R.; Thorsteinsson, T.; Werner, H.-J. *MOLPRO*; version 2002.6; 2004.
- (19) (a) Apra, E.; Bylaska, E. J.; Jong, W. d.; Hackler, M. T.; Hirata, S.; Pollack, L.; Smith, D.; Straatsma, T. P.; Windus, T. L.; Harrison, R. J.; Nieplocha, J.; Tipparaju, V.; Kumar, M.; Brown, E.; Cisneros, G.; Dupuis, M.; Fann, G. I.; Fruchtl, H.; Garza, J.; Hirao, K.; Kendall, R.; Nichols, J. A. K.; Tsemekhman Valiev, M.; Wolinski, K.; Anchell, J.; Bernholdt, D.; Borowski, P.; Clark, T.; Clerc, D.; Dachsels, H.; Deegan, M.; Dyall, K. D.; Elwood Glendening, E.; Gutowski, M.; Hess, A.; Jaffe, J.; Johnson, B.; Ju, J. R.; Kobayashi Kutteh, R.; Lin, Z.; Littlefield, R.; Long, X.; Meng, B. T.; Nakajima Niu, S.; Rosing, M.; Sandrone, G.; Stave, M. H.; Taylor, G.; Thomas Lenthe, J. v.; Wong, A.; Zhang, Z. *NWChem*, Version 4.7, 2006. (b) Kendall, R. A.; Apra, E.; Bernholdt, D. E.; Bylaska, E. J.; Dupuis, M.; Fann, G. I.; Harrison, R. J.; Ju, J.; Nichols, J. A.; Nieplocha, J.; Straatsma, T. P.; Windus, T. L.; Wong, A. T. *Comput. Phys. Commun.* **2000**, *128*, 260–283.
- (20) Woon, D. E.; Dunning, T. H., Jr. *J. Chem. Phys.* **1993**, *98*, 1358.
- (21) (a) Becke, A. D. *J. Chem. Phys.* **1993**, *98*, 5648. (b) Lee, C.; Yang, W.; Parry, R. G. *Phys. Rev. B* **1988**, *37*, 785.
- (22) Godbout, N.; Salahub, D. R.; Andzelm, J.; Wimmer, E. *Can. J. Chem.* **1992**, *70*, 560.
- (23) Shimanouchi, T. *Tables of Molecular Vibrational Frequencies, Consolidated Volume 1*, NSRDS NBS-39, U.S. Dept. Commerce: Washington D.C., 1972.
- (24) Peterson, K. A.; Woon, D. E.; Dunning, T. H., Jr. *J. Chem. Phys.* **1994**, *100*, 7410.
- (25) Rittby, M.; Bartlett, R. J. *J. Phys. Chem.* **1988**, *92*, 3033.
- (26) Knowles, P. J.; Hampel, C.; Werner, H.-J. *J. Chem. Phys.* **1994**, *99*, 5219.
- (27) Deegan, M. J. O.; Knowles, P. J. *J. Chem. Phys. Lett.* **1994**, *227*, 321.
- (28) (a) Peterson, K. A.; Dunning, T. H., Jr. *J. Chem. Phys.* **2002**, *117*, 10548. (b) Woon, D. E.; Dunning, T. H., Jr. *J. Chem. Phys.* **1993**, *98*, 1358.
- (29) Davidson, E. R.; Ishikawa, Y.; Malli, G. L. *J. Chem. Phys. Lett.* **1981**, *84*, 226.
- (30) Moore, C. E. *Atomic Energy Levels*; National Bureau of Standards Circular, Washington, D. C. 1949; 467.
- (31) (a) Ruscic, B.; Mayhew, C. A.; Berkowitz, J. *J. Chem. Phys.* **1988**, *88*, 5580. (b) Storms, E.; Mueller, B. *J. Phys. Chem.* **1977**, *81*, 318. Ochterski, J. W.; Petersson, G. A.; Wiberg, K. B. *J. Amer. Chem. Soc.* **1995**, *117*, 11299.
- (32) Curtiss, L. A.; Raghavachari, K.; Redfern, P. C.; Pople, J. A. *J. Chem. Phys.* **1997**, *106*, 1063.
- (33) Curtiss, L. A.; Raghavachari, K.; Redfern, P. C.; Rassolov, V.; Pople, J. A. *J. Chem. Phys.* **1998**, *109*, 7764.
- (34) Curtiss, L. A.; Redfern, P. C.; Raghavachari, K.; Rassolov, V.; Pople, J. A. *J. Chem. Phys.* **1999**, *110*, 4703.
- (35) Becke, A. D. *J. Chem. Phys.* **1993**, *98*, 5648–5652.
- (36) Hehre, W. J.; Radom, L.; Schleyer, P. R.; Pople, J. A. *Ab Initio Molecular Orbital Theory*; John Wiley and Sons: New York, 1986.
- (37) Squillacote, M.; Sheridan, R. S.; Chapman, O. L.; Anet, F. A. L. *J. Am. Chem. Soc.* **1975**, *97*, 3444–3446.
- (38) Dixon, D. A. *J. Phys. Chem.* **1990**, *94*, 5630.
- (39) Corfield, P. W. R.; Shore, S. G. *J. Am. Chem. Soc.* **1973**, *95*, 1480.
- (40) Halgren, T. A.; Anderson, R. J.; Jones, D. S.; Lipscomb, W. N. *J. Chem. Phys. Lett.* **1971**, *8*, 547.
- (41) Leavers, D. R.; Taylor, W. J. *J. Phys. Chem.* **1977**, *81*, 2257.
- (42) Harshbarger, W.; Lee, G.; Porter, R. F.; Bauer, S. H. *Inorg. Chem.* **1969**, *8*, 1683.
- (43) Duncan, J. L.; Mills, I. M. *Spectrochim. Acta* **1964**, *20*, 523.
- (44) Harmony, M. D.; Laurie, V. W.; Kuczowski Schwendeman, R. H.; Ramsay, D. A.; Lovas, F. J.; Lafferty, W. J.; Maki, A. G. *J. Phys. Chem. Ref. Data* **1979**, *8*, 619.
- (45) Grant, D. J.; Dixon, D. A. *J. Phys. Chem. A* **2006**, *110*, 12955.
- (46) Custelcean, R.; Jackson, J. E. *Chem. Rev.* **2001**, *101*, 1963.
- (47) Klooster, W. T.; Koetzle, T. F.; Siegbahn, P. E. M.; Richardson, T. B.; Crabtree, R. H. *J. Am. Chem. Soc.* **1999**, *121*, 6337.
- (48) Cramer, C. J.; Gladfelter, W. L. *Inorg. Chem.* **1997**, *36*, 5358.
- (49) Jacquemin, D.; Perpète, E. A.; Wathelet, V.; André, J.-M. *J. Phys. Chem. A* **2004**, *108*, 9616.
- (50) Li, J.; Kathman, S. M.; Schenter, G. K.; Gutowski, M. *J. Phys. Chem. A* **2007**, *111*, 3294.
- (51) Li, J. S.; Zhao, F.; Jing, F. Q. *J. Chem. Phys.* **2002**, *116*, 25.
- (52) Morrison, C. A.; Siddick, M. M. *Angew. Chem., Int. Ed.* **2004**, *43*, 4780.
- (53) Richardson, T. B.; de Gala, S.; Crabtree, R. H.; Siegbahn, P. E. M. *J. Am. Chem. Soc.* **1995**, *117*, 12875.
- (54) Niedenzu, K.; Sawodny, W.; Watanabe, H.; Dawson, J. W.; Totani, T.; Weber, W. *Inorg. Chem.* **1967**, *6*, 1453.
- (55) Kaldor, A.; Porter, R. F. *Inorg. Chem.* **1971**, *10*, 775.
- (56) Crawford, B. L., Jr.; Edsall, J. T. *J. Chem. Phys.* **1939**, *7*, 223.
- (57) T-Raissi, A. Technoeconomic Analysis of Area II Hydrogen Production Part II. *Proceedings of the 2002 U.S. DOE Hydrogen Program Review*; NREL/CP-610–32405, <http://www1.eere.energy.gov/hydrogenandfuelcells/pdfs/32405b15.pdf>. Shaulov, Y. K.; Shmyreva, G. O.; Tubyanskaya, S. Zh. *Fiz. Khim.* **1966**, *40*, 122; CAN 64:63834.
- (58) Baitalow, F.; Wolf, G.; Grolier, J. P. E.; Dan, F.; Randzio, S. L. *Thermochim. Acta* **2006**, *445*, 121.
- (59) Cramer, C. J. *Essentials of Computational Chemistry*; John Wiley & Sons: Chichester, U.K. 2002; pp 335, 336.
- (60) Hehre, W. J.; Ditchfield, R.; Radom, L.; Pople, J. A. *J. Am. Chem. Soc.* **1970**, *92*, 4796.
- (61) Redfern, P. C.; Zapol, P.; Curtiss, L. A.; Raghavachari, K. *J. Phys. Chem. A* **2000**, *104*, 5850.
- (62) Gilbert, T. M. *J. Phys. Chem. A* **2004**, *108*, 2550.
- (63) $S^{\circ}_{\text{expt}} - S^{\circ}_{\text{calc}} = 1.6(n - 3) - 0.2 \text{ cal}(\text{mol}\cdot\text{K})$ ($r^2 = 0.9998$) for C_3-C_6 linear alkanes using data for G3 method and experiment: *NIST Computational Chemistry Comparison and Benchmark Database, NIST Standard Reference Database*; Johnson, R. D., III, Ed.; August 2005; Number 101, Release 12, <http://srdata.nist.gov/cccbdb>.
- (64) Minkin, V. I.; Glukhovtsev, M. N.; Simkin, B. Y. *Aromaticity and Antiaromaticity*; Wiley: New York, 1994.
- (65) Dewar, M. J. S.; de Llano, C. *J. Am. Chem. Soc.* **1969**, *91*, 789.
- (66) Streitwieser, A.; Heathcock, C. H. *Introduction to Organic Chemistry*, 2nd ed.; Macmillan Publishing Co., Inc.: New York, 1981.
- (67) Han, S. S.; Kang, J. K.; Lee, H. M.; van Duin, A. C. T.; Goddard, W. A., III *J. Chem. Phys.* **2005**, *123*, 114703.
- (68) Zhang, J.; Zhang, S.; Li, Q. S. *J. Chem. Phys. Lett.* **2005**, *407*, 315.
- (69) Feyerisen, M. W.; Feller, D.; Dixon, D. A. *J. Phys. Chem.* **1996**, *100*, 2993.